

Determining optimum period of withholding irrigation for inducing maturity

Abstract

We report synthesis, characteristics and in vitro tests of folate-conjugated gold nanoparticles (AuNPs) and doxorubicin, having Cysteamine as linker. AuNPs were chemically synthesized using sodium citrate. Characterization was done using UV-visible absorption spectroscopy, Field Emission Gun Scanning Electron Microscopy (FEG-SEM), Fourier Transform Infra Red (FTIR) spectroscopy, Particle size Analyzer. Charge distribution was studied by recording Zeta potential. AuNPs were used for attaching folic acid through a linker cysteamine-HCl and finally preparing AuNP/Cysteamine-HCl/Folic acid/Doxorubicin complex. The cell cytotoxicity was studied in MDCK cells (normal cells) and HeLa cells (cancerous cells) having high level of folate receptor expression. In-vitro drug release kinetics was calculated using standard statistical models and was found to follow Hixson-Crowell drug release kinetics model.

Keywords: Cysteamine, Doxorubicin, Drug delivery, Folic acid, Gold nanoparticles, HeLa cells

Volume 1 Issue 1 - 2014

Roopa Dharmatti, Chinmay Phadke, Ashmi Mewada, Sunil Pandey, Goldie Oza, Chetna Sharon, Madhuri Sharon

N.S.N. Research Centre for Nanotechnology and Bionanotechnology (nsnRc), India

Correspondence: Madhuri Sharon, N.S.N. Research Centre for Nanotechnology and Bionanotechnology (nsnRc), Maharashtra, India, Tel 91-9552599207
Email sharonmadhuri@gmail.com

Received: September 04, 2014 | **Published:** September 16, 2014

Abbreviations: RES, Reticulo Endothelial System; FA, Folic Acid; FRs, Folic acid Receptors; AuNP, Gold nanoparticles; CYS, Cysteamine; DOX, Doxorubicin; DDC, Dicyclohexyl Carbodiimide; NHS, N-Hydroxy Succinimide; FEG-SEM, Field Emission Gun Scanning Electron Microscopy; DMSO, Dimethyl Sulfoxide; DLE, Drug Loading Efficiency

Introduction

The most jeopardizing situation of a transformed biological cell is its impenetrability of chemotherapeutic agent due to its high diffusion rate and enhanced reticuloendothelial system (RES) clearance. This physiological change poses a hostile consequence of low retention of the drugs inside a solid tumour.¹ This necessitates the development of tumour specific targeted drug delivery cargoes to ferry drugs, exploiting the leaky tumour microvasculature.² Nanomedicine plays a gigantic role in delivery of payloads to the target using specifically addressed nano-cargoes. Such nano-cargoes, due to size and surface properties can circumvent the problem of systemic toxicity of drugs. Moreover, they get anchored to certain tissues, thus decreasing the efficiency of diffusion and uniform tissue distribution. Targeting the nano-vehicle using the specific ligand facilitates balance between tissue penetration and cellular uptake leading to optimal therapeutic efficacy. Among the most pervasive diagnostic markers found on the surface of cancer cells, folic acid receptors occupy central position. Folic acid (FA) can act as targeting ligand for folate receptors which are over expressed on cancerous cells, and are internalized via receptor-mediated endocytosis facilitating cytosolic delivery of chemotherapeutic agent.³ Folic acid receptors (FRs) are prevalent on epithelial cancers of ovary, colon, lungs, prostate, throat and brain.^{4,5} FRs is also over expressed on hematopoietic malignancies of myeloid origin. They have got potential advantages over monoclonal antibodies, which includes; small size of the ligand often leading to desirable pharmacokinetic properties and reduced immunogenicity.

Gold nanoparticles (AuNP) are considered to be an attractive candidate for delivering plethora of payloads into the respective targets.⁶⁻⁹ They also exhibit distinct surface Plasmon resonance bands, making them suitable for easy characterization and incorporation

of functional ligands on the surface. Also, its size can be fine tuned during synthesis and its surface can be modified according to the chemistry of tethering molecule such as antibodies. Such surface orchestrated AuNPs can serve as a proficient candidate for payload of drug due to its long circulation time and low cytotoxicity.¹⁰⁻¹² For loading chemotherapeutic drug and conjugating antibodies, specific capping of the surface of AuNPs must be done using thiols, disulfides, and amines due to their strong binding affinities towards the surface of gold nanoparticles.¹³ Doxorubicin is the most widely used anti-cancer drug which acts against topoisomerases II, an enzyme in DNA replication and repair. The three main problems associated with cancer chemotherapy are: high toxicity, low retention of the drug and low solubility.¹⁴ These issues have exacerbated the delivery of active drugs to cancer cells. Hence, to overcome such problems, drug delivery vehicles like AuNPs, polymers like liposomes,¹⁵ hydro-gels to deplete the toxicity of drugs.

In our study, we orchestrated AuNPs with Cysteamine HCl (CYS) as a linker for synaptic drug delivery of doxorubicin using FA as navigating molecule. To best of our knowledge, there is no other evidence for using Cysteamine as a linker attaching doxorubicin. Apart from acting as ideal non-toxic linker, Cysteamine is an effective medicine for the treatment of lethal neurological disorders.¹⁶ Cysteamine also act as precursor of many vital components of the metabolic system such as synthesis of Coenzyme A, a cardinal evidence for its non-toxicity. Its cleavage product play critical role in combating with the disorders like cystinosis and cystinuria. Moreover, due to the presence of -SH, it becomes easy to attach Cysteamine on the surface of AuNPs and hence does not require pre-thiolation like polyethylene glycol. The molecular affinity of gold nanoparticles towards thiolated molecules is already taken into consideration. Thiol group can exchange sulphhydryl groups with surface cysteine of proteins in the blood, efficiently generating protein carrier conjugates with altered bioavailability and pharmacokinetic profiles. But, thiolated AuNPs are expected to be resistant to exchange with proteins due to the steric shielding of the gold thiol interface. Hence, DOX is attached to CYS functionalized AuNP along with FA as navigating molecule and In vitro drug release was studied using Zero order, First order, Higuchi and Hixson-Crowell pharmacokinetics models.

Materials and methods

Materials

Chloroauric acid (HAuCl_4 , Molecular Weight 393.79g mol), 1% Trisodium citrate ($\text{Na}_3\text{C}_6\text{H}_5\text{O}_7$), Folic acid, Dicyclohexylcarbodiimide (DDC), N-hydroxy succinimide (NHS), DMSO were purchased from Sigma Aldrich(USA). Cysteamine hydrochloride (CYS) was obtained from Merck, Germany. All the glass wares were washed with aqua regia and experiments were performed in nanopure water (18M Ω). MDCK and HeLa cell lines were procured from National center for cell sciences (NCCS, Pune). RPMI1640 without FA was purchased from Invitrogen Technologies (Carlsbad, CA). All the other chemicals used for experimental considerations were of high purity.

Synthesis of AuNPs

AuNPs were synthesized using Turkevich method.¹⁷ 30 μL solution of 0.25 M of gold chloride was added to 1% tri-sodium citrate in 14.22 mL of nano-pure water. The pH of the whole mixture was maintained 5 during the synthesis. The solution was boiled to 100°C, converting yellow colored gold solution to violet, blue and finally wine red color was obtained.

Analysis of synthesized AuNPs

Spectroscopic analysis of AuNP was performed using dual beam UV-Vis Spectrophotometer (Perkin-Elmer lambda 25) having path length of 1 cm. Morphological details of the synthesized AuNPs were studied using Field Emission Gun Scanning Electron Microscopy (FEG-SEM of Carl Zeiss Micro imaging GmbH, Germany). For sample preparation, 2–3 drops of the colloidal gold solution were dispensed onto a silicon wafer and dried under ambient condition before examination. Surface chemistry of the AuNP was studied using FTIR (alpha FT-IR spectrophotometer, Bruker optik GmBH, Germany). Particle size analysis and particle size distribution was performed using NanoSight LM20 (NanoSight, Amesbury, UK). The samples were injected into the sample chamber with sterile syringes (BD Discardit II, New Jersey, USA) until the liquid reached the tip of the nozzle. Zeta potential measurements were done using laser Doppler electrophoresis. All the measurements were performed at room temperature.

Synthesis of AuNP-CYS complex

For synthesis of the AuNP and CYS complex, 30 μL of 30 mM CYS was added in 10 mL of 9.770 mL of colloidal gold solution. The solution was sonicated for 3 hours and then centrifuged at 1500 rpm for 15 minutes. Supernatant was decanted and pellet was resuspended in dimethylsulfoxide (DMSO). Characterization of the complex was done using UV-Vis spectrophotometer, FTIR, Particle size analysis and Zeta potential measurements.

Activation of FA

Activation of the folic acid was carried out by dissolving 0.25 g of FA into 20 mL of DMSO and the mixture was subjected to sonication for 45 minutes. The carboxylate group of folic acid was activated by addition of 0.225 g of NHS and 0.125 g of DCC. The reaction was allowed to take place in inert environment created by argon gas at 28 \pm 2 °C for 12 hrs (FA/NHS/DCC molar ratio 2:2:1). The resultant mixture was filtered through Whatman filter paper and was used for further characterization.

Preparation of AuNP-CYS-FA Conjugate

The activated FA (1mL) was reacted with 9 mL of CYS decorated

AuNPs. The mixture was purged with argon with continuous stirring for 4 hours. The resultant solution was centrifuged and supernatant was diluted with nanopure water. The solution was further dialysed against nanopure water thrice (Molecular weight cut off: 1000). The purified complex was analysed using UV-vis spectrometer and FTIR.

Synthesis of AuNP-CYS-FA-DOX Conjugate

Doxorubicin was attached to AuNP-CYS-FA-DOX complex for destruction of cancer cells. Equimolar concentration of Doxorubicin (0.25mM) and AuNP-CYS-FA (0.25mM) were subjected to reduction with Triethylamine (0.5mM) and using DMSO as a solvent. The molar ratio of AuNP-CYS-FA/DOX/TEA was 1:1:2. The mixture was purged using Argon gas under continuous stirring at 50°C for 4 hours. The resultant AuNP-CYS-FA-DOX conjugate was purified using extensive dialysis against nanopure water for three days using a dialysis tubing (MW cut-off of 3000Da) to remove the excess amount of unbound DOX molecules and DMSO. The water was exchanged at 6h intervals. The whole complex was characterized using UV-vis Spectrophotometer, FTIR and Zeta potential measurement.

Drug loading efficiency calculations

From the total concentration of DOX used for attachment onto FA conjugated AuNP, some of it remains unattached. Hence, it becomes necessary to carry out an experiment for understanding the exact amount of drug that has actually got attached to AuNP.

Final conjugate was centrifuged at 5000 rpm and 5 mL of pallet resuspended in nano-pure water then was purified using 15kDa membrane against 150mL of nano-pure water for 24 hours. Unbound drug concentration was calculated using standard calibration curve of DOX (straight line equation $y=7.092x-0.014$) in case of centrifugation supernatant and dialysis which were further added. Drug loading efficiency was calculated using following equation:

$$DLE = \frac{\text{Theoretical amount of drug loaded} - \text{Free drug}}{\text{Theoretical amount of drug loaded} - \text{Free drug}} \times 100$$

In-vitro drug release studies

Cancerous cells exhibit a microenvironment which is acidic in nature when compared to that of inherent physiological pH i.e. 7.4. The bond formed between folate conjugated AuNP and DOX is expected to be pH dependent. Hence, amount of DOX released should vary according to pH variation in tumor microenvironment. Also during folate-mediated endocytosis, the pH of the formed endosome is approximately 5.3. This adds to the specificity and thus increasing the therapeutic index of DOX. 3mL dialyzed AuNP-CYS-FA attached DOX was placed in three different dialysis bags. The entire system was kept in incubator at 37°C in beaker containing 50 mL of phosphate buffer solution at pH 5.3. The drug release study was conducted with continuous stirring at 100 rpm. To measure the drug release content, samples (3 mL) were periodically removed and replaced with an equivalent volume of the phosphate buffer solution. The amount of released DOX was analyzed with a spectrophotometer at 485 nm and calculated using standard calibration curve of DOX in PBS ($y=6.572x+0.010$). Similarly drug release studies were also carried out at pH 6.8 and 7.4. The experiments were performed in triplicate for each of the samples and drug release kinetics was studied using Zero order, First order, Higuchi and Hixson-Crowell pharmacokinetics model according to our previous studies.^{18,19}

Cytotoxicity studies using MTT assay

Cytotoxicity of AuNPs, AuNPs-FA-DOX and DOX was determined using both MDCK cells and HeLa cells by MTT assay

which is based on the mitochondrial enzyme mediated conversion of pale yellow MTT to violet formazan crystals. Cells were then seeded in a 96 tissue culture well plate and cell concentration was adjusted to 5×10^5 cells/ml and incubated overnight at 37°C in a humidified incubator, 5% CO₂ (Galaxy 130, New Brunswick, Germany). On the next day, different concentrations of AuNPs and conjugate were added to the wells and again incubated for 8 to 10 hrs at 37°C in CO₂ incubator. After incubation, 10µl MTT reagent (5mg/ml) was added in each well and incubated at 37°C for 4 hrs in CO₂ incubator. After the incubation, 100 µl of 0.1 N acidified isopropanol was then added to each well and kept in dark for 30 min at RT. The well plates were then kept on a shaker for 1 min and intensity of violet color was read at 570 nm wavelength.

Results and discussion

Synthesized gold nanoparticles

Synthesis of AuNPs using Turkevich method lead to formation of stable and monodispersed nanoparticles, showing Surface Plasmon Resonance at 525 nm (Figure 1a) which is further confirmed by FEG-SEM representing monodispersed spherical AuNPs of diameter 2-10 nm (Figure 2a). The appearance of the wine red color becomes more intense when the de-broglie wavelength of the valence electrons becomes equal to or less than the size of the particle.²⁰ Due to this phenomenon the freely mobile electrons are caged in gold nanoparticles and exhibit a characteristic collective coherent oscillation of Plasmon resonance giving rise to surface Plasmon resonance (SPR) in the range of 500-600 nm depending on the size and shape of the AuNP (Figure 1a).

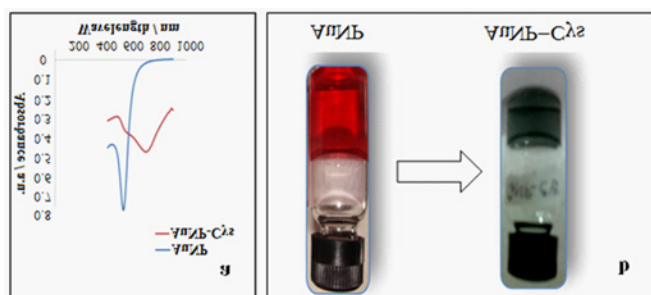


Figure 1

- UV-Vis spectra showing a shift in the surface plasmon resonance of AuNPs due to adsorption of CYS.
- Change in the color of colloidal AuNP from red to grayish blue after formation of the AuNP-CYS complex.

After addition of the varying concentration of CYS, it was determined that 25mM CYS concentration was found to prevent the agglomeration of AuNP. Cysteamine diminishes the agglomeration by acting as thermodynamically efficient capping agent, thereby stabilizing the surface energy of AuNP.²¹ The interaction of Cysteamine with Gold NP leads to the red shift in surface plasmon resonance peak (Figure 1a). As a consequence, the change in colour of the AuNP-CYS conjugate occurs (Figure 1b). The reason behind this alteration in color may be due to the change in the particle size and alteration in the refractive index of the medium or in the peripheral region of the particle.²¹ The adsorption of CYS on the surface of AuNPs may also perturb the electron density into the metal nanoparticle and consequently changing the interaction with the light, a phenomenon which brings change in the SPR band (Figure 1a). Diffraction (SAED) pattern further indicates that the particles are face-centred cubic structured (FCC) which has (1, 1, 1) twin planes (Figure

2b). Nanoparticle Tracking Analysis measurements for Particle size distribution of AuNP exhibited size range between 2-10 nm (Figure 2c). Figure 2d depicts a 3D graph (size vs. intensity vs. concentration) of average data further confirms the AuNP size range distribution.

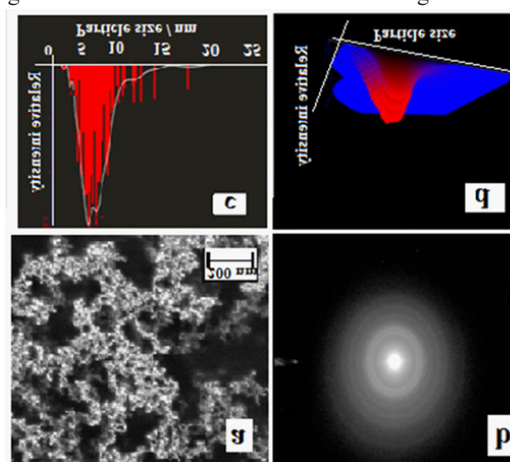


Figure 2

- FEG-SEM of AuNPs showing spherical AuNPs with size range of 2-10nm diameter.
- SAED pattern shows particles that are face-centred cubic which has (1, 1, 1) twin planes.
- Tracking analysis measurements for Particle size distribution of AuNP exhibiting size range between 2-10nm.
- Normalized 3D graph (size vs. intensity vs. concentration).

FTIR analysis

FTIR spectra of AuNP displayed in (Figure 3a), represented a minor peak at C-Cl stretch of halides due to precursor used in AuNP synthesis i.e. HAuCl₄. A minor peak at 1025 cm⁻¹ and medium intensity peak at 1453 cm⁻¹ correspond to C-O stretch of alcohol and CH₂ bend of alkanes. A medium intensity peak at 1595 cm⁻¹ depicts C=C stretch of aromatics. A medium intensity peaks at 171.01 cm⁻¹ and sharp peak at 2856.58 cm⁻¹ corresponds to C=O stretch of and C-H stretch of aldehyde respectively. An intense and narrow peak at 2922.94 cm⁻¹ indicated C-H stretch of alkanes. Broad and feeble peaks at 3466.53 cm⁻¹ and 3651 cm⁻¹ was due to -OH stretching of water molecules present in the sample in which AuNPs have been synthesized.

Figure 3b displayed FTIR spectra of AuNPs-CYS-FA complex. The peak at 837 cm⁻¹ and 665 cm⁻¹ interpreted as S=O stretching indicates that AuNPs has been thiolated by -SH group of CYS. Moreover, both the spectra of AuNPs-CYS-FA complex and Cysteamine (Figure 3c) show N-H bending at 1636 cm⁻¹. Further, the bands at 939 and 888 cm⁻¹ correspond to the bending of -NH₂ of CYS. The capping of AuNPs using thiol ligands desirably protects the surface, decreasing the entropy due to the partial liberation of the salvation shell and exchange reactions happening due to the displacement of carboxylic acid with the thiol group. This exchange reaction is relatively lucid procedure in which we presume that, it proceeds to completion. Owing to the strength of gold-thiol, it is being considered that exchange of thiolated ligands on AuNPs with other thiolated ligands is a more reluctant reaction, but has been widely exploited biologically.^{1,2} The existence of the band at 1407cm⁻¹ relates to asymmetric stretching vibration of -NH₂ in folate as its signature marker. The strong signal at 3428 cm⁻¹ is due the coupling of hydroxyl stretching. The disappearance of the band at 1713 cm⁻¹ (Figure 4a), which is the signature marker of the stretching vibration of C=O (carboxylic acids) and appearance of bending vibration at 823cm⁻¹ of N-H verifies that, there is formation

of amide linkage between activated FA and CYS. However, it must be noted that, folate has α and γ carboxylic acids and can be activated by DCC/NHS in the presence of Dimethylsulfoxide. It's a well known fact that γ carboxylic acids primarily get activated due to its higher reactivity.^{22,23} Hence, we speculate conjugation of α carboxylic group of folic acid with amino group of cysteamine.

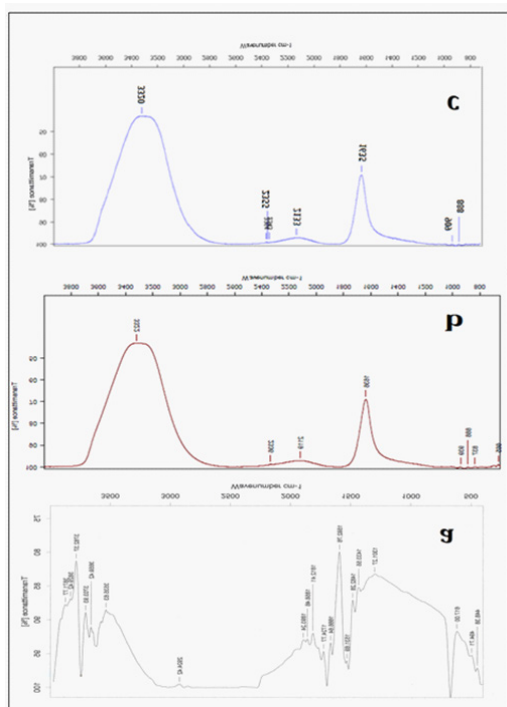


Figure 3 FTIR spectra of a. AuNP; b. AuNP-CYS-FA conjugate; c. CYS.

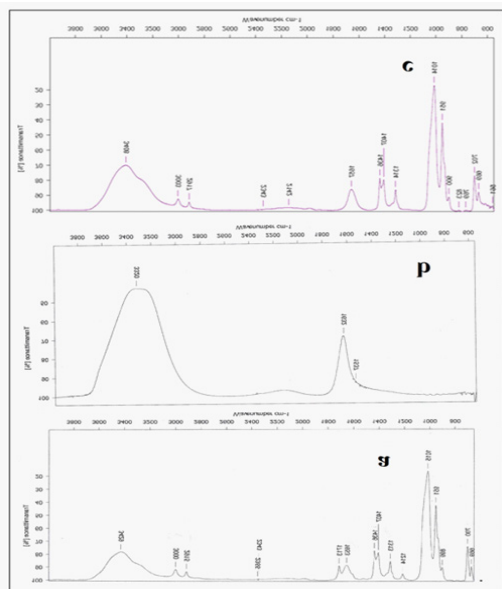


Figure 4 FTIR spectra of a. Activated FA; b. DOX; c. AuNP-CYS-FA-DOX complex.

FTIR spectra of DOX displays bands at 609 cm^{-1} and 752 cm^{-1} which arise from alkane CH_2 bends, alkene C-H bends and aromatic C-H bends. The prominent peak at 1603 cm^{-1} is due to aromatic C-C stretch and amine N-H bending vibrations in the molecule (Figure 4b). The emergence of weak bands at 561 cm^{-1} and 823 cm^{-1} in the FTIR spectra of AuNPs-Cys-FA-DOX complex (Figure 4c) correspond to bending vibration of C-H and bending vibration of N-H in amides respectively.

Zeta potential analysis

Figure 5 displayed the Zeta potential measurements of AuNPs and its complexes. AuNPs showed zeta potential value as -0.42 mV as the consequence of negative charge imparted by citrate capping on AuNPs. After conjugation with CYS, there was rise in Zeta potential value -19 mV due to interaction of thiol groups and AuNPs, thereby exposure of new groups on resultant complex. Moreover the Zeta potential value of final complex i.e. AuNP-CYS-FA-DOX was observed to be 18 mV due to inherent positive charge of DOX.

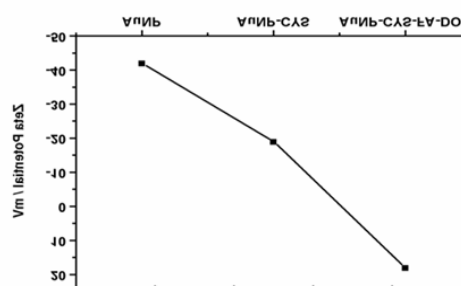


Figure 5 Zeta potential values of AuNP, AuNP-CYS and AuNP-CYS-FA-DOX conjugate.

Drug loading efficiency & Drug release studies

Biochemical properties of tumors^{24,25} including deformed layers of extracellular matrix and acidic environment turn out to be major limitation for drug delivery to solid tumors. Accessibility of anticancer drugs such as DOX has been hindered by enhanced interstitial fluid pressure imparted by alterations in tumor microenvironment. Such circumstances can be resolved with fabrication of smallest nanoparticle which is able to hold high quantity of drugs and deliver it to cancerous cells. In our case, CYS functionalized AuNPs when complied with DOX for synaptic DOX delivery. The amount of drug loaded onto AuNPs is 0.2296 mM and DLE was observed as 91.84% .

The Drug release was studied at pH 5.3, 6.8 and 7.4. Once the DOX conjugated AuNPs are internalized in cells through the endocytosis process, they encounter a series of endocytic compartments with increasing acidity. The acidic environment triggers the rapid release of DOX from its nano-carrier after they are internalized into tumor cells, thereby greatly enhancing the cells' Cytotoxicity.

Figure 6a showed the DOX release profile from the DOX conjugated AuNPs in phosphate buffer solution with pH values of 5.3, 6.8 and 7.4. Till 3 hours steady release of drug was observed, whereas, at the end of 4 hours, 12.98% and 20.12% of DOX was released in pH 5.3 and 7.4 respectively, while only 5.88% was released in pH 6.8. More amount of drug release was achieved at pH 7.4 followed by at pH 5.3 due to intrinsic characteristic pH dependent cleavable property of DOX molecules and AuNPs. After 24 hours at pH 5.3 and 7.4, there was rapid increase in the % release of drugs where, 25.48% and 32.67% drug was released respectively. Sensitivity towards both acidic and basic pH is an added advantage for tumor chemotherapy.

Table 1 showed Regression coefficient (R^2 values of different pharmacokinetic models at different pH. R^2 value is determinant of drug release nature offered by AuNP-CYS-FA-DOX complex. The DOX follows Hixson-Crowell model as highest R^2 value (0.9757) was obtained with this profile (Figure 6b). Drugs with such type of release profile show drug release through diffusion²⁶ and change in surface properties of nano conjugate as a function of time representing sustained drug release. Depending upon spatial distribution of tumors

from blood vessels, it can possess a range of pH values, which makes delivery and release of drugs difficult. In this scenario, nano-complex which can release drug at acidic as well as physiological pH serves important role. Thus, AuNP-CYS-FA-DOX complex is biggest contender for the delivery of anti-cancer drug.

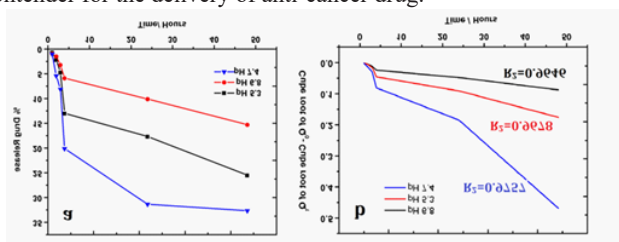


Figure 6

- Percentage drug release in In vitro with respect to time
- Drug release profile of DOX following Hixson-Crowell release kinetics.

Table 1 R2 value for different pharmacokinetic models at different pH.

	pH 5.3	pH 6.8	pH 7.4
Zero Order	0.9417	0.9527	0.9229
First Order	0.9745	0.9692	0.9367
Higuchi	0.9672	0.9716	0.9681
Hixson-Crowell	0.9678	0.9646	0.9757

Cytotoxicity

As mentioned earlier, HeLa cells express maximum concentration of FA receptors which are used in drug targeting in case of tumor cells. In absence of FA, only AuNPs could not easily get internalized into the HeLa and MDCK cells. AuNPs are found to be biocompatible against both cells, as percentage viability of MDCK and HeLa cells were 50.5% and 49.3% at their highest concentration respectively (Figure 7a & 7b). On the other hand, AuNP-CYS-FA-DOX conjugate showed highest cytotoxicity to HeLa cells and comparatively less toxicity to MDCK cells, as percentage viability of MDCK and HeLa cells were 31.2% and 13.4% respectively at their highest concentration. HeLa cells over expresses FRs, hence FA navigated conjugate get internalized effortlessly into HeLa cells. Free DOX could not differentiate between HeLa cells and MDCK cells, it was observed as highly cytotoxic to both cells (Figure 7a & 7b). Subsequently, targeting with FA proved to be important in differentiating cancerous cells from non cancerous cells.

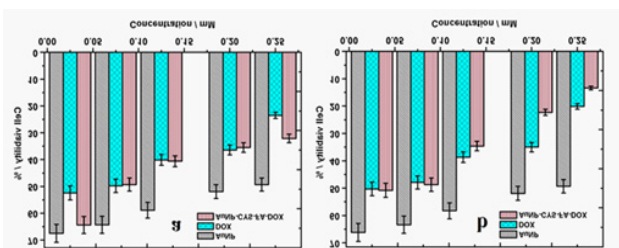


Figure 7 Cytotoxic effects of AuNP, DOX, AuNP-CYS-FA-DOX on a. MDCK and b. HeLa cells.

Conclusion

Monodispersed, small spherical AuNPs were synthesized using simple Turkevich and anchored with CYS which acted as linker for attachment of DOX. Hence, high drug loading capacity (~92%) was achieved. AuNP-CYS-FA-DOX conjugate showed ideal drug release profile at physiological as well as acidic pH and found to follow

Hixson-Crowell drug release profile based on statistical calculations. AuNPs were biocompatible on both cells. Only AuNP-CYS-FA-DOX showed higher Cytotoxicity towards cancer cells than free DOX and was less toxic to normal cells due to targeting molecule FA.

Acknowledgements

Authors are indebted to funding authorities of N.S.N. Research Centre for carrying out the projects. We are also thankful to TIFR, Mumbai and IIT Bombay, SAIF department-Mumbai for their support in FTIR and FE-SEM characterization.

Conflicts of Interest

None.

References

- Ali Mansoori G, Brandenburg KS, Shakeri-Zadeh AA comparative study of two folate-conjugated gold nanoparticles for cancer nanotechnology applications. *Cancers (Basel)*. 2010;2(4):1911-1928.
- Ali Mansoori G, Mohazzabi P, McCormack P et al. Nanotechnology in cancer prevention, detection and treatment: bright future lies ahead. *World Review of Science, Technology and Sustainable Development*. 2007;4(2-3):226-257.
- Kamen BA, Capdevila A Receptor-mediated folate accumulation is regulated by the cellular folate content. *Proc Natl Acad Sci USA*. 1986;83(16):5983-5987.
- Mattes MJ, Major PP, Goldenberg DM, Dion AS et al. Patterns of antigen distribution in human carcinomas. *Cancer Res*. 1990;50(3 Suppl):880S-884S.
- Ross JF, Chaudhuri PK, Ratnam M Differential regulation of folate receptor isoforms in normal and malignant tissues in vivo and in established cell lines. Physiologic and clinical implications. *Cancer*. 1994;73(9):2432-2443.
- Lee K, Lee H, Bae KH, Park TG Heparin immobilized gold nanoparticles for targeted detection and apoptotic death of metastatic cancer cells. *Biomaterials*. 2002;31(25):6530-6653.
- Hirsch LR, Stafford RJ, Bankson JA et al. Nanoshell-mediated near-infrared thermal therapy of tumors under magnetic resonance guidance. *Proc Natl Acad Sci USA*. 2003;100(23):13549-13554.
- Alivisatos AP, Gu W, Larabell C Quantum dots as cellular probes, *Annu Rev Biomed Eng*. 2005;7:55-76.
- Patra CR, Bhattacharya R, Mukhopadhyay D, Mukherjee P Application of gold nanoparticles for targeted therapy in cancer. *J Biomed Nanotechnol*. 2008;4(2):99-132.
- Paciotti GF, Myer L, Weinreich D et al. Colloidal gold: a novel nanoparticle vector for tumor directed drug delivery. *Drug Deliv*. 2004;11(3):169-83.
- Hong R, Han G, Fernandez JM et al. Glutathione-mediated delivery and release using monolayer protected nanoparticle carriers. *J Am Chem Soc*. 2006;128(4):1078-1079.
- Paciotti GF, Kingston DGI, Tamarkin L Colloidal gold nanoparticles: a novel nanoparticle platform for developing multifunctional tumor-targeted drug delivery vectors. *Drug Dev Res*. 2006;67(1):47-54.
- Perez-Juste J, Pastoriza-Santos I, Liz-Marzan LM et al. Gold nanorods: Synthesis, Characterization and applications. *Coordination Chemistry Reviews*. 2005;249(17-18):1870-1901.
- Dixit V, Bossche JV, Sherman DM et al. Synthesis and grafting of thioctic acid PEG-folate conjugate on to Au nanoparticles for selective targeting of folate receptor-positive tumor cells. *Bioconjug Chem*. 2006;17(3):603-609.

15. Lu Y, Low PS Folate-mediated delivery of macromolecular anticancer therapeutic agents. *Adv Drug Deliv Rev.* 2002;54(5):675–693.
16. Borrell-Page M, Canals JM, Cordelieres FP et al. Cystamine and cysteamine increase brain levels of BDNF in Huntington disease via HSJ1b and transglutaminase. *J Clin Invest.* 2006;116(5):1410–1424.
17. Turkevich T, Stevenson PC, Hillier J A Study of the Nucleation and Growth Processes in the Synthesis of Colloidal Gold. *Discussions of the Faraday Society.* 1951;11:55–75.
18. Pandey S, Shah R, Mewada A et al. Gold nanorods mediated controlled release of doxorubicin: nano-needles for efficient drug delivery. *J Mater Sci Mater Med.* 2013;24(7) 1671–1681.
19. Sunil P, Goldie O, Ashmi A et al. Folic acid mediated synaphic delivery of doxorubicin using biogenic gold nanoparticles anchored to biological linkers. *J Mater Chem B.* 2013;9:1361–1370.
20. Daniel MC, Astruc D Gold nanoparticles: assembly, supramolecular chemistry, quantum-size-related properties, and applications toward biology, catalysis and nanotechnology. *Chem Rev.* 2004;104(1):293–346.
21. Sardar R, Funston AM, Mulvaney P, Murray RW Gold nanoparticles: past, present, and future. *Langmuir.* 2009;25(24):13840–13851.
22. Wang S, Lee RJ, Mathias CJ, Green MA, Low PS (1996) Synthesis, purification and tumor cell uptake of 67Ga–deferoxamine–folate, a potential radiopharmaceutical for tumor imaging. *Bioconjug Chem.* 2009;7(1):56–62.
23. Wang S, Luo J, Lantrip DA et al. Design and synthesis of [111In]DTPA–folate for use as a tumor–targeted radiopharmaceutical. *Bioconjug Chem.* 1997;8(5):673–679.
24. Hobbs SK, Monsky WL, Yuan F et al. Regulation of transport pathways in tumor vessels: role of tumor type and microenvironment. *Proc Natl Acad Sci USA.* 1998;95(8):4607–4612.
25. Jain RK, Stylianopoulos T Delivering nanomedicine to solid tumors. *Nat Rev Clin Oncol.* 2010;7(11):653–664.
26. Sahoo SK, Sahoo SK, Behera A et al. Formulation In vitro drug release study and anticancer activity of 5–Fluorouracil loaded gellan gum microbeads. *Acta Pol Pharm.* 2013;70(1):123–127.